Journal of Quantitative Spectroscopy & Radiative Transfer 198 (2017) 141–144

Contents lists available at ScienceDirect

Journal of Quantitative Spectroscopy & Radiative Transfer

journal homepage: www.elsevier.com/locate/jqsrt

Infrared absorption cross sections of propane broadened by hydrogen

A. Wong[a,*], R.J. Hargreaves[b], B. Billinghurst[c], P.F. Bernath[a]

[a] Department of Chemistry and Biochemistry, Old Dominion University, Norfolk, VA, USA 23529
[b] Current address: Atmospheric, Oceanic & Planetary Physics, University of Oxford, Clarendon Laboratory, Parks Road, Oxford, OX1 3PU, UK
[c] Canadian Light Source Far-Infrared Beamline, 44 Innovation Blvd, Saskatoon, Canada SK S7N 2V3

ARTICLE INFO

Article history:
Received 4 March 2017
Revised 8 May 2017
Accepted 8 May 2017
Available online 10 May 2017

Keywords:
Absorption cross-sections
Fourier transform infrared
Propane
Giant planets
Synchrotron radiation

ABSTRACT

Fourier transform infrared absorption cross-sections of pure propane (C_3H_8) and propane broadened with H_2 have been calculated from transmittance spectra recorded at temperatures from 292 K to 205 K. Transmittance spectra were recorded at the Canadian Light Source (CLS) Far-Infrared beamline, utilizing both the synchrotron source and the internal glowbar source. The absorption cross-sections have been calibrated to Pacific Northwest National Laboratory (PNNL) reference cross-sections of propane and can be used to interpret astronomical observations of giant planets such as Jupiter and Saturn as well as exoplanets.

© 2017 Elsevier Ltd. All rights reserved.

1. Introduction

Propane is one of the many small hydrocarbons found in the Earth's atmosphere. The main source of atmospheric propane is fugitive emissions associated with oil and gas production with minor sources from biomass burning, oceans and volcanoes [1]. As a constituent of natural gas, it can be used to distinguish urban emissions from those due to oil and gas operations [2]. Although propane does not have a large direct radiative forcing, monitoring of atmospheric propane is still relevant because of its production of CO_2 and tropospheric O_3. In the troposphere, propane has a relatively long lifetime (about 14 days) and is oxidized by hydroxyl radicals into acetone and acetaldehyde [3,4]. This leads to the production of peroxyacetyl nitrate (PAN), which can transport NO_2 molecules over large distances; NO_x catalyzes the formation of tropospheric ozone [5,6].

The C-H stretching modes of propane, centered around 2963 cm^{-1} (3.37 μm), are the most intense bands of propane [7,8] and serendipitously, their absorption coincides with a He-Ne laser line at 3.39 μm [9]. As a result, it is possible to use He-Ne laser absorption spectroscopy to measure properties of propane such as its absorption coefficient [10,11] and concentration [12] in a fuel combustion environment. Absorption cross sections of propane at elevated temperatures and pressure have also been recorded [13,14] for the purpose of quantifying propane in combustion engines. Recently a set of high resolution pure propane cross sections were recorded at high temperatures [15] aimed at astronomical applications such as spectral analysis of the auroral regions of Jupiter.

The detection of propane is not just limited to Earth's atmosphere. In our Solar System, propane has been found in the atmospheres of the gas giant Saturn [16,17] and its moon Titan [18,19]. Propane is formed by hydrocarbon photochemistry starting from methane, e.g. [20]. Beyond our Solar System, gaseous propane has not yet been detected however there is a possibility of its existence in the atmospheres of cool brown dwarfs [21] and exoplanets as the presence of methane [22] in these objects has already been observed.

Propane has an equilibrium structure with C_{2v} symmetry and has 27 fundamental vibrational modes. Several of these vibrations have frequencies < 1500 cm^{-1} and only a few have been rotationally analyzed thus far by Fourier transform infrared (FTIR) spectroscopy: ν_9 (369 cm^{-1}) [23], ν_{21} (921 cm^{-1}) [24], ν_{26} (745 cm^{-1}) and $2\nu_9$-ν_9 (370 cm^{-1}) [25]. There are also two low frequency torsional modes (approximately 217 cm^{-1} and 265 cm^{-1} [26]) from the two methyl rotors which have been analyzed using microwave and submillimeter wave techniques [27]. At warm (even cold) temperatures, the torsional levels are highly populated and result in numerous hot bands that have appreciable intensities. These hot bands add to the spectral congestion and complexity of propane's gas phase spectrum, hindering the analysis when attempting to assign transitions and fit spectroscopic constants.

In the absence of accurate spectroscopic constants, absorption cross-sections provide an alternative method of using high quality laboratory data of "heavy" molecules. Absorption cross-sections

* Corresponding author.
E-mail address: awong@odu.edu (A. Wong).

http://dx.doi.org/10.1016/j.jqsrt.2017.05.006
0022-4073/© 2017 Elsevier Ltd. All rights reserved.

Table 1
Experimental conditions used for the individual scans.

1.066 kPa H_2 & C_3H_8				4 kPa H_2 & C_3H_8			
P (Pa)[a]	P_{eff} (Pa)[b]	T (K)	No. of scans	P (Pa)[a]	P_{eff} (Pa)[b]	T (K)	No. of scans
26.66	26.35	208.95	340	76.79	81.78	208.95	306
31.73	30.83	232.35	400	106.39	110.29	232.45	300
58.40	51.82[c]	262.15	406	101.72	109.35	262.15	300
71.33	67.43	291.85	344	115.86	115.87	292.35	311
13.33 kPa H_2 & C_3H_8				Pure Propane			
P (Pa)[a]	P_{eff} (Pa)[b]	T (K)	No. of scans	P (Pa)[a]	P_{eff} (Pa)[b]	T (K)	No. of scans
162.65	162.01	232.45	300	11.20	7.11[c]	204.35	104
146.25	144.05	262.35	300	31.73	30.17	231.95	266
173.32	169.45	292.15	300	40.93	38.15	262.55	156
				43.86	42.28	291.05	300
				46.00	51.12[c]	294.75	288

[a] The pressure given in these columns refers to the pressure of C_3H_8 used.
[b] Effective pressures after normalization.
[c] Although included here, these cross sections are not usable as large pressure calibrations are required.

do not rely on accurate fits of spectroscopic parameters, rather only physical conditions such as temperature, pressure and sample transmittance. Another advantage of absorption cross-sections is that they are directly relatable to what is observed in substellar environments such as cool brown dwarfs, exoplanets and other planetary objects [15,28]. Spectroscopic data for propane is also available in several databases such as HITRAN [29] and GEISA [30], however these sources are more applicable to Earth's atmosphere rather than those of other planets. We present here infrared absorption cross-sections of pure, and H_2 broadened, propane as cold as 200 K.

The work is part of a program to record spectra of small hydrocarbons with H_2, He and N_2 broadeners as needed for the analysis of cool astronomical objects. In another experiment, spectra have been recorded at temperatures below 200 K to better match the stratospheric temperatures of Jupiter and Saturn. In this first paper, however, we present the warmer propane cross sections. We note that temperatures above 200 K can be found in the thermosphere and troposphere of the giant planets as well as in auroral regions.

2. Experimental

Propane (C_3H_8) (99.99% purity) and H_2 (99.99% purity) were purchased from Praxair and used without further purification and we assume the isotopic contamination of ^{13}C to be approximately 1.1% according to its natural abundance. Depending on the conditions, either pure C_3H_8 (or a C_3H_8-H_2 mixture) was used in a multipass White cell set to an optical path length of 8 m (base path length = 2 m) that was operated in a static mode [31].

The cell temperature was either left at ambient temperature (approximately 298 K) or cooled to temperatures as low as 205 K using a NESLAB ULT-80DD refrigerated re-circulating methanol bath [32–34]. Once the cell had reached the desired temperature, it was left to equilibrate overnight and monitored with PT100 RTD sensors. Fluctuations in temperature during each experiment were ±0.1 K. The spectrometer was fitted with a KBr beamsplitter and a liquid He-cooled Ge: Cu detector was used for optimum sensitivity between 600 – 1250 cm^{-1}. Table 1 summarizes the individual conditions used for each experiment. Experiments with H_2 as the foreign broadening gas were carried out first by filling the cell with a small amount of propane and then adding H_2 to reach total pressures of 8 Torr (1.066 Pa), 30 Torr (4 kPa) and 100 Torr (13.33 kPa) determined using two baratron gauges (MKS 626B13TBE up to 1000 Torr and Micro Precision 627B11TEV1B up to 10 Torr) with estimated uncertainties of ±0.4 Pa.

Table 2
Observed full-width half-maximum linewidths (FWHM) near 700 cm^{-1} for unblended lines and the resolution used to record the spectra.

H_2 (kPa)	Obs FWHM (cm^{-1})	Resolution (cm^{-1})	
		Sample	Background
Pure (n/a)	0.002	0.00096	0.01536
1.066	0.01	0.005	0.04
4	0.035	0.01	0.04
13.33	0.1	0.04	0.04

For scans with pure propane, the full resolution of the spectrometer was utilized (0.00096 cm^{-1}) along with the synchrotron radiation as the light source. For H_2-broadened spectra, the resolution was reduced to match the increasing linewidths and the source changed to the internal glowbar mid-IR source (Table 2). This is because the advantages of the synchrotron source (being a near pinpoint source, having both higher flux and higher signal-to-noise) are lost with increasing aperture size. Furthermore, signal-to-noise levels are increased with decreasing resolution and the efficiency of recording scans is increased. Forward and reverse pairs of interferograms were recorded and saved as individual files before being Fourier transformed. During the Fourier transform, a Blackman-Harris 3-Term apodization function and a zero-fill factor of eight were used. Zero-filling serves to mitigate the picket fence effect from the fast Fourier transform process by adding additional data points to interpolate between the sampled points. This results in smoother spectra with more accurate line positions, intensities and areas.

Background spectra were recorded before and after each sample and the single channel profiles were then co-added using a weighted average. The most suitable background was used in order to obtain the final transmission spectrum.

3. Results and discussion

3.1. Cross-Sections

Fig. 1 provides a series of vertically offset C_3H_8 absorption cross-sections (σ_{CLS}) broadened by approximately 1.066 kPa (8 Torr) of H_2 at progressively decreasing temperatures ranging from 292 K to 209 K in the 650 – 1250 cm^{-1} region. The absorption

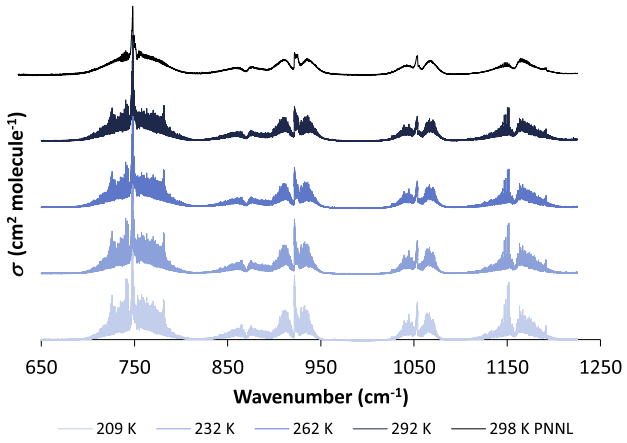

Fig. 1. σ_{CLS} (bottom four blue) and σ_{PNNL} (top black trace) of C_3H_8 broadened by 4 kPa of H_2 at four different temperatures (298 K–209 K). (Color plot with online version) "(For interpretation of the references to color in this figure legend, the reader is referred to the web version of this article.)".

cross-section of C_3H_8 from the Pacific Northwest National Laboratory (σ_{PNNL}) at 298 K is also included for reference [35]. Pure C_3H_8, and all H_2-broadened σ_{CLS} were calculated from transmission spectra using Eq. (1) [7] and can be found in the supplementary data [36]:

$$\sigma(\nu,T)_{CLS} = -\xi\frac{10^4 k_B T}{Pl}\ln\tau(\nu,T) \quad (1)$$

where σ is the cross-section (cm^2 molecule^{-1}), ξ[1] is the calibration factor, ν is the frequency (in cm^{-1}), k_B is the Boltzmann constant (J K^{-1}), T is the temperature (K), P is the pressure (Pa), l is the optical pathlength (m) and τ is the transmittance at a given (ν, T).

Since the C_3H_8 σ_{PNNL} are in units of ppm^{-1} m^{-1}, it was necessary to re-calculate the σ_{PNNL} in order to give consistent units of cm^2 molecule^{-1} using the factor, $F = 9.28697 \times 10^{-16}$, obtained from:

$$F = \frac{k_B \times T \times \ln(10) \times 10^4}{0.101325} \quad (2)$$

with T = 296 K. By doing so, it is then possible to directly compare the integrated σ_{PNNL} and σ_{CLS} values (cm molecule^{-1}) in order to verify the accuracy of our measurements (Eq. (3)).

$$\int_{970cm^{-1}}^{680cm^{-1}} \sigma(\nu,T)_{PNNL}d\nu \approx \int_{970cm^{-1}}^{680cm^{-1}} \sigma(\nu,T)_{CLS}d\nu \quad (3)$$

The lower integration limit of 680 cm^{-1} was chosen due to the low wavenumber cut-off of the Ge: Cu detector, whereas the upper integration limit of 970 cm^{-1} was used as there are no C_3H_8 absorption features in this region (see Fig. 1). When integrating over the whole region (i.e. 650 – 1250 cm^{-1}) there are inconsistences between the three σ_{PNNL} (278, 298 and 323 K) absorption cross-sections: 7.716×10^{-19}, 9.641×10^{-19} and 9.137×10^{-19} cm^2 molecule^{-1} respectively. Because of this, both the lower and upper integration limits were restricted to achieve a more reliable result. Furthermore, only the σ_{PNNL} from the 298 K was used as a reference for this work. This reduced integration range gave more reliable integrated σ_{CLS} and σ_{PNNL} values and is reflected in the P_{eff} values provided in Table 1. Almost all of the P_{eff} values fall within 10% of the observed pressures during the measurement.

[1] ξ is used to compensate for the difficulty in accurately determining the amount of absorbing gas by normalizing the σ_{CLS} to the σ_{PNNL} values.

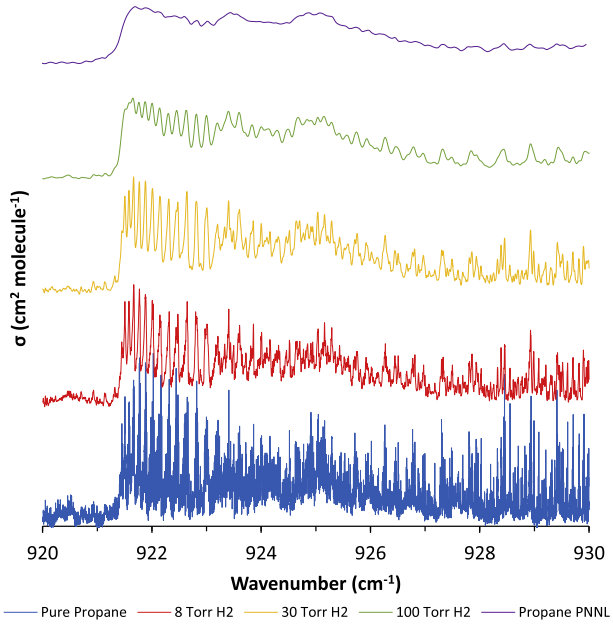

Fig. 2. A section of the σ_{CLS} (292 K) (bottom four traces) and σ_{PNNL} (top trace) between 920–930 cm^{-1} with increasing H_2 broadening gas pressure. (Color plot with online version) "(For interpretation of the references to color in this figure legend, the reader is referred to the web version of this article.)".

A small section showing the Q-branch structure near 922 cm^{-1}, as a function of increasing pressure from the H_2 broadening gas is presented in Fig. 2. As the amount of foreign H_2 broadening gas is increased, the sharp and intense Q-branch structure broadens and becomes less intense, forming a pseudo continuum. The integrated area remains constant as the intense individual lines broaden and merge into a weaker continuum resulting in integrated σ_{CLS} values that are all consistent throughout all temperature and pressure series. At these temperatures and high pressures, overlapping ro-vibrational lines make it almost impossible to assign transitions and accurately fit spectroscopic constants. This further demonstrates the robust nature of using absorption cross-sections for astronomical spectroscopy in the absence of accurate line parameters.

4. Conclusions

Spectra of cold and ambient temperature C_3H_8 have been recorded in the 650 – 1250 cm^{-1} region. C_3H_8 has been measured as a pure sample as well as broadened with varying pressures of H_2. The individual absorption cross-sections have been calculated and calibrated to a reference cross-section obtained from the PNNL spectroscopic database.

These cold absorption cross-sections are relevant for planetary atmospheres, where the physical conditions and composition differ from that of the Earth. The absence of high quality spectroscopic line parameters necessitates the use of absorption cross sections in the retrieval of abundances of molecules such as propane in planetary atmospheres and bypass the need to assign transitions and fit spectroscopic constants. Our absorption cross sections can be point-by-point interpolated in both temperature and H_2 pressure to obtain a suitable cross section within the laboratory measurement range.

In the low frequency region of the IR, a synchrotron source is advantageous over conventional laboratory based sources such as a glowbar. This is especially true when taking advantage of the full resolution of the spectrometer for samples at low pressure. Syn-

chrotron radiation provides a near point source with high brightness leading to a higher signal-to-noise ratio and thus increased sensitivity. However, when recording spectra of high pressure samples at lower resolution, it is more efficient to use the internal source as the synchrotron loses its brightness advantage with increasing aperture size.

Acknowledgments

We could like to thank the NASA (grant nos. NNX13AK95G and NNX16AG44G) Outer Planets Research and Planetary Data Archiving and Restoration Tools programs for funding. Research described in this paper was performed at the Canadian Light Source, which is supported by the Canada Foundation of Innovation, Natural Sciences and Engineering Research Council of Canada, the University of Saskatchewan, the Government of Saskatchewan, Western Economic Diversification Canada, the National Research Council Canada, and the Canadian Institutes of Health Research.

References

[1] Pozzer A, Pollmann J, Taraborrellii D, Jöckel P, Helmig D, Tans P, et al. Observed and simulated global distribution and budget of atmospheric C_2-C_5 alkans. Atmos Chem Phys 2010;10:4403–22.
[2] Gilman JB, Lerner BM, Kuster WC, de Gouw KA. Source signature of volatile organic compounds from oil and natural gas operations in Northeastern Colorado. Environ Sci Technol 2013;47:1297–305.
[3] Rosado-Reyes CM, Francisco JS. Atmospheric oxidation pathways of propane and its by-products: acetone, acetaldehyde, and propionaldehyde. J Geophys Res 2007;112 D14310.
[4] Singh HB, O'Hara D, Herlth D, Sachse W, Blake DR, Bradshaw JD, et al. Acetone in the atmosphere: distribution, sources, and sinks. J Geophys Res 1994;99:1805–19.
[5] Fischer EV, Jacob DJ, Yantosca RM, Sulprizio MP, Millet DB, Mao J, et al. Atmospheric peroxyacetyl nitrate (PAN): a global budget and source attribution. Atmos Chem Phys 2014;14:2679–98.
[6] Kanakidou M, Singh HB, Valentin KM, Crutzen PJ. A two-dimensional study of ethane and propane oxidation in the troposphere. J Geophys Res 1991;96:15395–413.
[7] Harrison JJ, Bernath PF. Infrared absorption cross sections for propane (C_3H_8) in the 3 μm region. J Quant Spectrosc Radiat Transfer 2010;111:1282–8.
[8] Kondo S, Saëki S. Infrared absorption intensities of ethane and propane. Spectrochim Acta 1978;29A:735–51.
[9] Jaynes DN, Beam BH. Hydrocarbon gas absorption by a HeNe Laser beam at 3.39 μm wavelength. Appl Opt 1969;8:1741–2.
[10] Tsuboi T, Inomata K, Tsunoda Y, Isobe A, Nagaya K. Light absorption by hydrocarbon molecules at 3.392 mm of He-Ne laser. Jpn. J. Appl. Phys. 1985;24:8–13.
[11] Tomita E, Kawahara N, Nishiyama K, Shigenaga M. *In situ* measurement of hydrocarbon fuel concentration near a spark plug in an engine cylinder using the 3.392 μm infrared laser absorption method: application to an actual engine. Meas Sci Technol 2003;14:1357–63.
[12] Yoshiyama S, Hamamoto Y, Tomita E, Minami K. Measurement of hydrocarbon fuel concentration by means of infrared absorption technique with 3.39 μm HeNe laser. JSAE Rev 1996;17:339–45.
[13] Klingbeil AE, Jeffries JB, Hanson RK. Temperature- and pressure-dependent absorption cross sections of gaseous hydrocarbons at 3.39 μm. Meas Sci Technol 2006;16:1950–7.
[14] Mével R, Boettcher PA, Shepherd JE. Absorption cross sections at 3.39 μm of alkanes, aromatics and substituted hydrocarbons. Chem Phys Lett 2012;531:22–7.
[15] Beale CA, Hargreaves RJ, Bernath PF. Temperature-dependent high resolution cross sections of propane. J Quant Spectrosc Radiat Transfer 2016;182:219–24.
[16] Guerlet S, Fouchet T, Bézard B, Simon-Miller AA, Flasar FM. Vertical and meridional distribution of ethane, acetylene and propane in Saturn's stratosphere from CIRS/Cassini limb observations. Icarus 2009;203:214–32.
[17] Greathouse TK, Lacy JH, Bézard B, Moses JI, Richter MJ, Knez C. The first detection of propane on Saturn. Icarus 2006;181:266–71.
[18] Roe HG, Greathouse TK, Richter MJ, Lacy JH. Propane on Titan. Astrophys J 2003;597:L65–8.
[19] Nixon CA, Jennings DE, Flaud J–M, Bézard B, Teanby NA, Irwin PGJ, et al. Titan's prolific propane: the Cassini CIRS perspective. Planet Space Sci 2009;57:1573–85.
[20] Cheng L, Zhang X, Gao P, Yung Y. Vertical distribution of C_3-hydrocarbons in the stratosphere of Titan. Astrophys J Lett 2015;803 L19.
[21] Cushing MC, Rayner JT, Vacca WD. An infrared spectroscopic sequence of M, L and T dwarfs. Astrpphys J 2005;623:1115–40.
[22] Swain MR, Vasisht G, Tinetti G. The presence of methane in the atmosphere of an extrasolar planet. Nature 2008;452:329–31.
[23] Tchana FK, Flaud J–M, Lafferty WJ, Manceron L, Roy P. The first high-resolution analysis of the low-lying ν_9 band of propane. J Quant Spectrosc Radiat Transer 2010;111:1277–81.
[24] Perrin A, Tchana FK, Flaud J–M, Manceron L, Demaison J, Vogt M, et al. First high resolution analysis of the ν_{21} band of propane $CH_3CH_2CH_3$ at 921.382 cm^{-1}: evidence of large amplitude tunnelling effects. J Mol Spectrosc 2015;315:55–62.
[25] Flaud J–M, Tchana FK, Lafferty WJ, Nixon CA. High resolution of the ν_{26} and $2\nu_9$-ν_9 bands of propane: modelling of Titan's infrared spectrum at 13.4 μm. Mol Phys 2010;108:699–704.
[26] Grant DM, Pubmire RJ, Livingston RC, Strong KA, McMurray HL, Brugger RM. Methyl libration in propane measured with neutron inelastic scattering. J Chem Phys 1970;52:4424–36.
[27] Drouin BJ, Pearson JC, Walters A, Lattanzi V. THz measurements of propane. J Mol Spectrosc 2006;240:227–37.
[28] Sung K, Toon GC, Mantz AW, Smith MAH. FT-IR measurements of cold C_3H_8 cross sections at 7-15 μm for Titan atmosphere. Icarus 2013;226:1499–513.
[29] Rothman LS, Gordan IE, Babikov Y, Barbe A, Benner DC, Bernath PF, et al. The HITRAN2012 molecular spectroscopic database. J Quant Spectrosc Radiat Transfer 2013;130:4–50.
[30] Jacquinet-Husson N, Armante R, Scott NA, Chédin A, Crépeau L, Boutammine C. The 2015 edition of the GEISA spectroscopic database. J Mol Spectrosc 2016;327:31–72.
[31] Johns JWC, Lu Z, McKellar ARW. Infrared Spectrum of the CO-Xe van der Waals Complex. J Mol Spectrosc 1993;159:210–16.
[32] Dawadi MB, Twagirayezu S, Perry DS, Billinghurst BE. High-resolution Fourier transform infrared spectroscopy of the NO_2 in-plane rock of nitromethane. J Mol Spectrosc 2015;315:10–15.
[33] McKellar ARW, Billinghurst BE. High-resolution synchrotron infrared spectroscopy of thiophosgene: the ν_1, ν_5, $2\nu_4$, and $\nu_2+\nu_6$ bands. J Mol Spectrosc 2015;315:24–9.
[34] McKellar ARW, Billinghurst BE. High-resolution synchrotron infrared spectroscopy of acrolein: the vibrational levels between 700 and 820 cm^{-1}. J Mol Spectrosc 2015;315:41–5.
[35] Sharpe SW, Johnson TJ, Sams RL, Chu PM, Rhoderick GC, Johnson PA. Gas-phase databases for quantitative infrared spectroscopy. Appl Spectrosc 2004;58:1452–61.
[36] Insert link for supplementary data. Note: The total size of all supplementary files exceeded the 700 MB limit and were not uploaded onto EVISE. They are available upon request with the corresponding author and from P. Bernath.